Xanthan Gum Recovery from Palm Oil-Based Fermentation Broth by Hollow Fibre Microfiltration (MF) Membrane with Process Optimisation Using Taguchi Method

M. Sufian So'aib[a,*], M. Sabet[b], J. Krishnan[a], and M. VPS Veluri[c]

[a]Faculty of Chemical Engineering, Universiti Teknologi MARA (UiTM), 40000 Shah Alam, Selangor, Malaysia

[b]Chemical Engineering Department, Universiti Teknologi PETRONAS, Bandar Seri Iskandar, 31750 Tronoh, Perak, Malaysia

[c]School of Science and Engineering, Manipal International University, MAS Academy, No. 2, Jalan SS7/13, Kelana Jaya, 47301 Petaling Jaya, Selangor, Malaysia

Original scientific paper
Received: March 13, 2012
Accepted: January 11, 2013

First stage Xanthan recovery (cell and oil separation) from palm oil-based fermentation broth was carried out by hollow fibre microfiltration (MF) using Taguchi method as design of experiment (DOE) to study the effect of four main parameters on Xanthan recovery; transmembrane pressure (TMP), crossflow velocity (CFV), ionic strength (IS) and temperature (T). From S/N ratio larger-the-better analysis, optimum conditions for Xanthan recovery were at level 2 of TMP, IS and T respectively and level 1 for CFV whereas the significance of factor found by ANOVA was in the following order: IS > TMP > T > CFV. Confirmation experiment based on optimum condition yield 64 % Xanthan recovery. Particle size was influenced by intramolecular and intermolecular interactions of Xanthan's side chain under varying pH and cation concentration and affected the degree of Xanthan's transmembrane transport (XTT). Interpretation of zeta potential (ZP) elucidated XTT mechanism driven by surface charge modification of membrane surface due to cation binding. The formation of oily cake layer hindered most XTT, whereas better XTT achieved for zero-oil broth filtration.

Key words:
Microfiltration, Xanthan's transmembrane transport, Taguchi method

Introduction

Xanthan gum is a secretion product of bacterium Xanthamonas Campestris[1] and widely used as stabilising agent in cosmetic, beverage, food and pharmaceutical products[2] as well as drilling fluid in oil extraction.[3]

Accumulation of Xanthan during fermentation in stirred-tank bioreactor leads to high broth viscosity which creates caverning phenomenon i.e. well-mixing region around impeller but stagnant fluid beyond this region which is detrimental to oxygen transfer to suspended cells throughout the tank.[4] Consequently, Xanthan yield was limited to only 2.5 % w/v. Previously, cell immobilisation was expected to improve oxygen transfer by direct aeration to cells residing on fixed bed, but poor oxygen transfer was also encountered upon scale-up and Xanthan build up.[5]

In the past several years, studies on biphasic broth have circumvented the viscosity problem without entirely replacing the traditional stirred-tank bioreactor by distributing the viscosity across broth volume by confining the Xanthan gum in aqueous droplets dispersion in continuous vegetable oil phase i.e. water-in-oil (W/O) system.The benefit of W/O system can be seen from the reported increase of Xanthan yield per volume of aqueous medium. Maximum cell of concentration 13 g L^{-1} (per aqueous volume) was obtained using perfluorocarbon (PFC) as organic phase compared to 3 for all aqueous broth under similar condition. This entailed 50 g L^{-1} of Xanthan yield compared to 25 g L^{-1} of the conventional system. More recently, improved cell growth and Xanthan yield; 16 and 100 respectively was observed by using vegetable oil as continuous phase in oil-in-water (O/W) broth system.

Despite successful studies on Xanthan yield improvement by W/O broth, a comprehensive recovery method received little attention. Thus, conventional recovery method is likely chosen as a downstream method for these studies i.e. centrifugation and alcohol precipitation. However, a major issue with conventional downstream method is

*Corresponding author, Tel.:+6013 7955248; Fax: +603 55436300; E-mail address: sufian_sj@yahoo.com

high production cost attributed to energy intensive centrifugation and massive amount of alcohol for cell and Xanthan separation respectively which contributes to 60 % of overall production cost[7]. It is also unclear how oil components can be effectively separated from the broth to ensure the purity of the purified Xanthan. On the other hand, membrane filtration has been used widely in the separation of several bioproducts from fermentation broth such as surfactin (biosurfactant)[8], fumaric acid[9], alginate[10], penicillin G[11], enzymes[12] and protein[13]. In those applications, membranes were used to concentrate the final product (dewatering), typically by ultrafiltration (UF) or nanofiltration (NF). There were a few studies which employed two steps microfiltration (MF) and UF/NF in series to carry out cell separation at MF stage followed by product's concentration at UF/NF.[14] With regard to oil separation, membrane filtration is used in demulsification of (W/O) effluent.[15,16]

Nevertheless, concentration polarisation and fouling remain a drawback for membrane filtration application[17] which put additional cost on intensive cleaning and eventual membrane replacement.[18] These drawbacks are influenced by physico-chemical of membrane-solute and solute-solute interactions.[19] Thus operating parameters must be optimized to minimise the occurrence of concentration polarisation and fouling. The optimum condition stands on a particular combination of operating parameters' value, but finding the optimum combination from several parameters such as transmembrane pressure (TMP), crossflow velocity (CFV), temperature and solution chemistry is a cumbersome process. In trial and error approach, a parameter is varied while the rest is kept constant until all possible combinations are tested. If there are four parameters each at three different values; the total number of possible combinations is $3^4 = 81$ whereas the interaction between parameters is not possibly determined. Fortunately, Taguchi's orthogonal array (OA) allows the experimenter to vary all factors simultaneously and determine the effect of each factor from a small number of experiments whereas interaction between factors can be determined from OA's linear graph.[20,21]

In this study, the feasibility of MF to separate Xanthan gum from palm oil-based fermentation broth was investigated. The effect of four main parameters; TMP, CFV, temperature and ionic strength on Xanthan permeation and process optimisation were carried out using Taguchi method. Taguchi's results were later elucidated by particle size distribution (PSD) analysis, zeta potential (ZP) and fouling analysis.

Material and method

Xanthan gum production

Xanthan was produced by fermentation in palm oil-based fermentation broth using the method described elsewhere.[22] The fermentation was carried out in 50 % oil fraction in a 7-l bioreactor (INFORS HT) with 4.5-l working volume.

Membrane

Hollow fibre polysulfone MF membrane was purchased from General Electric (GE). It had an effective surface area of 420 cm^2 (0.042 m^2) and the following dimensions; 30 cm length, 1.0 mm internal diameter and 1.9 mm outer diameter.

Experimental setup

The lab-scale membrane filtration unit was fabricated from polypropylene pipe, digital flow meter (Burkert), stainless steel pressure gauge (Burkert) and manual polypropylene diaphragm valve (Burket). The schematic diagram of crossflow filtration unit is shown in Fig. 1. Broth solution was held in 1L beaker placed on hot plate (brand) equipped with magnetic stirrer and heat regulator and was diluted 10 times prior to experiment. Desired TMP was obtained by adjusting the valves fitted at the feed outlet and membrane module's outlet (retentate) while leaving permeate valve fully opened i.e. zero pressure. The corresponding pressure at each point was measured by pressure gauge. TMP was calculated as follows:

$$TMP = \frac{P_{Feed} + P_{R\,etentate}}{2} - (P_{Permeate} = 0) \quad (1)$$

Fresh membrane was rinsed thoroughly by NaOH solution (0.2 M) for 1 hour to remove storage agent, followed by distilled water for another

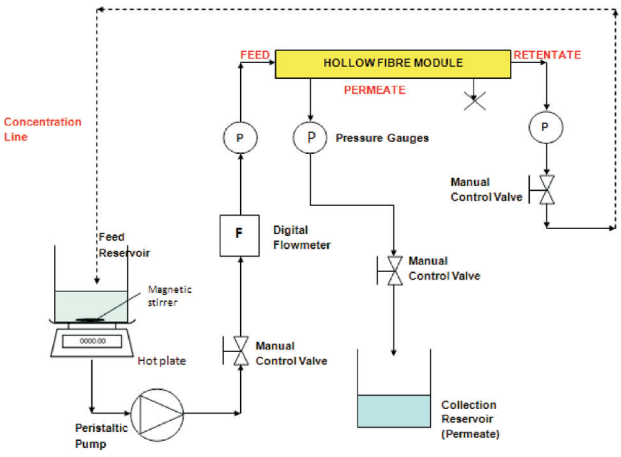

F i g . 1 – *Lab scale MF Hollow fibre crossflow filtration unit*

1 hour. Then the initial pure water flux (J_w) was determined from Darcy's equation:

$$J_w = \frac{1}{A}\frac{\mathrm{d}V}{\mathrm{d}t} \tag{2}$$

where A is effective membrane area m^2, V is permeate volume m^3 and t is filtration time s.

The experiments were carried out in concentration mode where permeate yield was collected in separate container whereas retentate was recirculated to the feed tank.

Analytical methods

Determination of Xanthan concentration

Xanthan concentration was determined by dry weight method. Cells were separated by centrifugation at 12 000 rpm for 15 minutes. The supernatant was precipitated by isopropanol (IPA) at volume ratio IPA:supernatant of 3:1. The precipitate was dried overnight in an oven at temperature 60 °C and weighed. The Xanthan separation/recovery (*%R*) was calculated as follows:

$$\%R = \frac{C_P}{C_F} \times 100\% \tag{3}$$

where C_P is Xanthan concentration in permeate, C_F is Xanthan concentration in initial feed.

Measurement of membrane resistance

Total resistance (R_t) was calculated using Darcy's law for constant transmembrane pressure i.e.:

$$J(t) = \frac{TMP}{\mu(t)R_t} \tag{4}$$

where $J(t)$ is flux, $\mu(t)$ is permeate viscosity ($Pa\ s$).

Determination of fouling mechanism

Fouling mechanism was determined by plotting the total resistance vs. filtration time based on resistance-in-series (RIS) model;[23]

$$R_t = R_m(1 + 4tK_{CF}Q_0^2)^{0.5} \tag{5}$$

Measurement of viscosity

The apparent viscosity of Xanthan was determined by a viscometer (LVDV-II + PRO Brookfield) equipped with small sample adaptor and spindle SCA-18 at 100 rpm or shear rate 132 s^{-1}. This shear rate was chosen because previously significant effect of Xanthan concentration was not observed at shear rate less than 0.1 s^{-1} or greater than 1000 s^{-1}.[24]

Estimation of conductivity and zeta potential

Conductivity and zeta potential was estimated by laser Doppler velocimetry and phase analysis light scattering (PALS) in combination with patented M3-PALS techniques based on the principle of particle's electrophoretic mobility using Malvern's Nano ZS instrument. Sample was filled into a folded capillary cell (Malvern's DTS1060) prior to analysis.[25]

Estimation of particle size distribution (PSD)

Particle size distribution (PSD) was estimated by dynamic light scattering (DLS) technique using Malvern's Nano ZS equipped with 633 nm wavelength laser emission. The detector's scattering angle was set at 90° and connected to digital correlator. Maximum count rate was set at 2000 s^{-1}. Sample was filled into a folded capillary cell (Malvern's DTS1060) prior to analysis. PSD was given in terms of hydrodynamic diameter based on particle translational diffusion across the fluid in reference to equivalent diameter of sphere having similar translational diffusion speed of the particle. Particle sizes were differentiated based on the intensity of scattered light; larger particles scattered more light and vice versa. Fluctuating intensity over time was measured by digital correlator and later fitted into correlation function to yield an apparent particle size in terms of mean size (z-average diameter) or PSD. To appreciate the particle's occupancy using Mie theory, intensity distribution was converted to volume distribution. Data analysis was analysed using Zetasizer software v. 6.20.

Measurement of pH

The pH of the sample was measured by pH meter, routinely calibrated at pH 4 and pH 7.

Determination of oil presence

The permeate quality in terms of oil presence was analysed by gas chromatography (GC) equipped with mass spectrometer (MS) detector. A fused silica capillary column of 30 m × 0.32 mm ID, film thickness 0.25 μm was installed. The oven temperature was programmed as follow: 80 °C hold for 2 minutes at 20 °C min^{-1} until 125 °C (hold for 1 minute), then raised to 220 °C (hold for 3 minutes) at 3°C min^{-1}. The injector and detector were operated at 240 °C. Nitrogen was used as carrier gas at flow rate of 1 ml/minute and a split ratio of 1:10 was applied. Pure palm oil was used as standard. Each pure oil sample, initial feed sample and permeate sample was mixed with hexane in 2 ml sample cells to dissolve palm oil residue.

Design of experiment (DOE) method

Four main operating factors studied; TMP, CFV, IS and T are given in Table 1. KCl was used to vary ionic strength.

Table 1 – *Operating parameters and levels*

Parameters	Level		
	1	2	3
A. TMP, Transmembrane pressure (bar)	0.6	1.0	1.4
B. CFV, Crossflow velocity (ml min^{-1})	1.0	1.5	2.0
C. IS, Ionic strength (M)	0.2	0.5	0.8
D. T, Temperature (°C)	40	60	80

Taguchi's L_9 orthogonal array (OA) was chosen for the above experimental conditions since it has degree of freedom (*DOF*) greater or at least equal to the DOF of above experimental design. The L_9 (3^4) OA shown in Table 2 contains nine randomised experimental trials. Xanthan recovery was chosen as its quality characteristic (response).

Experimental result was analysed by signal-to-noise (S/N) ratio which measured the deviation of result from the desired value. S/N ratio larger-the-better (SN_L) was chosen as performance indicator since maximum Xanthan recovery is desirable. SN_L is defined as follows:[26]

$$S/N = -10\log\left(\frac{1}{n}\sum_{i=1}^{n}\frac{1}{y_i^2}\right) \quad (6)$$

where n is the number of repetition, y_i is the response's value at ith trial.

Table 2 – *Result from L_9 (3^4) Taguchi's orthogonal array*

Trial	Factors and levels				Response (%R)			Ω (db)		SN_L
	A	B	C	D	1	2	average	1	2	
1	1	1	1	1	2.71	13.12	7.92	–15.55	–8.21	20.23
2	1	2	2	2	6.41	6.41	6.41	–11.64	–11.64	21.32
3	1	3	3	3	22.8	7.44	15.14	–5.29	–10.95	16.56
4	2	1	2	3	1.29	9.68	5.49	–18.84	–9.7	21.72
5	2	2	3	1	6.56	16.9	11.73	–11.54	–6.92	18.47
6	2	3	1	2	2.31	5.91	4.11	–16.26	–12.02	22.72
7	3	1	3	2	9.4	17.6	13.23	–9.84	–6.7	17.88
8	3	2	1	3	27.7	16.74	22.2	–4.18	–6.97	14.09
9	3	3	2	1	4.7	10.92	7.81	–13.07	–9.12	20.48

Confirmation result based on optimum level of each factor determined by S/N ratio should agree with calculated optimum response (Y_{opt}) within a chosen confidence interval (CI) to validate Taguchi method. Y_{opt} is calculated using the following additivity equation, taking only significant factors:

$$Y_{opt} = \overline{T} + (\overline{A}_i - \overline{T}) + (\overline{C}_j - \overline{T}) + (\overline{D}_k - \overline{T}) \quad (7)$$

where $\overline{T}$ is average of all performance results (recovery), $\overline{A}_i, \overline{C}_j$ and $\overline{D}_k$ are average response of the significant factors at their respective optimum level i, j, k etc.

Confidence interval is calculated by the following equation:

$$CI = \pm\sqrt{(F(1, n_2) \times v_e / N_e)} \quad (8)$$

where $F(1, n_2)$ = The F value from the F Table at the required confidence level at DOF 1 and error DOF n_2

v_e = variance of error term (from ANOVA)

$$N_e = \frac{\text{Total number of results (or number of S/N ratios)}}{\text{DOF of mean (=1, always) + DOF of all factors included in the estimate of mean}}$$

Percentage values were converted into omega terms using omega transformation equation (equation 9) before applying equations (6) and (7). Conversion of percentage value into omega term was necessary to avoid misinterpretation of additivity result when the data has poor additivity e.g. if percentage value is very close to 0 % or 100 %.[27]

$$\Omega = -10\log\left(\frac{1}{p} - 1\right) \quad (9)$$

where p is fractional value of percentage (e.g. p = 0.58 = 58 %)

Results in terms of S/N ratio and omega must be converted back to original terms (percentage) at the end of analysis.

Result and discussion

Taguchi results

The result of Xanthan recovery based on Taguchi's experimental design is shown in Table 2. The effect of factor on Xanthan recovery can be seen from the mean S/N ratio plot for each level of factor shown in Fig. 2 where the highest peak indicates optimum condition. The different degree of S/N ratio variation of each factor signifies different degree of influence of the factor on the response e.g. IS showed greater S/N ratio variation compared

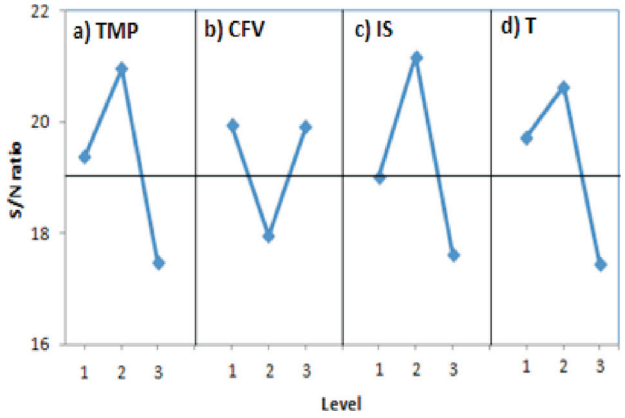

F i g . 2 – *Main effect S/N plot for Xanthan recovery a) TMP b) CFV c) IS d) T*

to CFV indicating the former's greater effect on the response.

Effect of TMP

The highest S/N ratio of TMP was observed at middle range i.e. 1.0 bar whereas the lowest S/N ratio was at the highest TMP i.e. 1.4 bar (Fig. 2). Although flux and XTT may be enhanced at higher TMP, earlier study found that the benefit of higher TMP was likely for operation below critical flux i.e. before solute's concentration polarisation phenomenon occurred.[28] Hence at level 3 of TMP, greater driving force for particle deposition on membrane surface probably shifted the flux to its critical point leading to concentration polarisation and cake layer formation, which quickly turned higher TMP into disadvantage due to increased osmotic pressure acting in the opposite direction of TMP. Previous study found transmembrane mass transport eventually became TMP-independent if aforementioned phenomenon prolonged,[29] thus causing XTT in this study less likely.

Nevertheless, higher TMP was favourable to encourage oil droplets coalescence so that oil retention by membrane surface occurred more easily.[30, 31] However, oil dispersion in this study was unstable i.e. coalescence and subsequent aqueous-oil phase separation could occur near-spontaneously, thus rendering higher TMP non-critical. All of these justified the optimum moderate TMP as the most favourable condition for XTT while minimising the formation of concentration polarization and cake layer.

Effect of CFV

The highest S/N peak for CFV was observed at the highest level. CFV commonly reduces Xanthan viscosity by shear-thinning[24] and creates hydrodynamic force and turbulence to disrupt concentration polarisation and cake layer.[31] However, the insignificance of varying CFV displayed by S/N ratio plot was due to the presence of complex, multi-component cake layer structure comprising microbial cells, oil and Xanthan. Xanthan molecule, being several orders smaller than membrane's pore size blocked the pore to cause internal fouling, preventing any permeation of incoming Xanthan whereas other feed components contributed to the forming of external fouling layer. The minimal effect of CFV was not surprising as particle size-dependence of Xanthan permeation would immediately ceased by even the slight formation of fouling layer or partial blocking of membrane pores, despite the fact that high CFV could remove some degree of cake layer.

Effect of IS

The optimum level of ionic strength was observed at moderate concentration i.e. 0.5 M. The large variation of S/N ratio suggested significant ionic strength influence on solute-solute and solute-membrane interaction which later affected XTT. This was no surprise since Xanthan is highly electric-charged due to the carboxylic group attached to its glucoronic and pyruvate side chains and displays anionic character at neutral pH.[7] Such property contributed to the dynamic of molecular conformation when subjected to various cation concentration.[32] At low ionic strength, earlier study reported the repulsion between negatively charged side chain groups which caused Xanthan's helical structure to unwind resulting in a more random and linear structure. This was the likely condition of Xanthan structure at 0.5 M ionic strength where its solubility was maximum and most permeable to microfiltration pores and porous cake layer. This is supported by the fact that interaction between Xanthan's side chain with its backbone structure was a strong function of ionic strength[32] in which a suitable ionic concentration could shield Xanthan's intramolecular repulsion to obtain more permeable, smaller size sphero-colloidal particle. Excessive ionic strength, i.e. 0.8 M in this case, shielding effect by cation might have neutralised the repulsive interaction between functional groups of neighbouring Xanthan molecules resulting in flocculation which also known as salting-out effect.[29,33] This hampered further particle size-dependence of XTT thus contributing to rapid concentration polarisation. Likewise, similar effect of ionic strength on integrity of cake layer formed by microbial cells had been reported i.e. low ionic strength allows greater repulsive electrical double layer, keeping individual cell far apart thus minimising the tendency to aggregate.[34] Conversely, extremely high cation concentration contributed to closed-packed arrangement of cells in gel layer.[35] There was the possibility that cell's

cake layer in this study could have been consolidated by Xanthan deposition which filled the void and sealed the remaining gaps for Xanthan permeation.

Effect of temperature

The optimum temperature was observed at moderate level of 60 °C. Several studies agreed that higher temperature reduced overall solution viscosity and increased molecular diffusion[16, 36] whereas others reported thermal expansion of pore membrane which unfavourably susceptible to in-pore blocking.[37] In this study, the former effect could encourage XTT whereas the latter could cause pore plugging, thus plausibly explaining why the lowest S/N ratio was observed at the highest temperature as such condition was unfavourable to XTT. Therefore, moderate temperature of 60 °C was optimum because it allowed solute's mass transport whilst not causing excessive thermal pore expansion which could render the membrane more susceptible to pore plugging.

ANOVA results

ANOVA results in Table 3 show the contribution of each factor to the response. Factor B i.e. CFV which had the least contribution and was later pooled as error term. The statistical significance of every factor was determined by F ratio which was defined as the ratio of factor's variance to error's variance. A factor is statistically significant at chosen confidence level if its F-ratio is larger than critical F-ratio (F_{cr}). For a factor having DOF = 2 and error's DOF = 2, F_{cr} at 95 % confidence level is 19 but none of the factors fulfilled this condition in order to be statistically significant i.e. the variance of factor was not statistically significant compared to variance of error in order to cause a meaningful effect on the response (recovery) at the selected confidence level. Nevertheless, the reliability of the experimental result was founded upon the contribution of error, which at 12.69 % was well below 50 % maximum error limit, thus implying the insignificance of experimental error. The significance of each factor was ranked according to its percent contribution i.e. IS > TMP > T > CFV.

Table 3 – *Pooled ANOVA result for Xanthan Recovery*

Factor	SS	DOF	v	F-ratio	F_{cr}	%P
A	18.27	2	9.13	2.35	19	29.85
B	(7.77)	(2)		Pooled		
C	19.08	2	9.54	2.46	19	31.17
D	16.09	2	8.05	2.07	19	26.29
Error	7.77	2	3.88			12.69
Total	61.20	8				100

Confirmation experiment

Confirmation experiment was conducted based on optimum condition determined by S/N ratio to validate Taguchi's methodology. Confirmation experiment results agreed with the optimum prediction at 5 % error as shown in Table 4.

Table 4 – *Optimum condition of parameters and observed, predicted and confidence interval of Xanthan recovery*

Parameters	Optimum working condition	
	Value	Level
TMP, Transmembrane Pressure (bar)	1.0	2
CFV, Crossflow velocity	1.0	1
IS, Ionic strength (M)	0.5	2
T, Temperature (°C)	60	2
Observed recovery (%)	64.21	
Predicted recovery (%)	97.70	
Predicted confidence interval (%)	64–100	

Particle size distribution (*PSD*) *analysis*

Relatively higher Xanthan recovery observed in trial 3 and 8 can be attributed to their smaller particle size at retentate side as shown in Table 5. This agreed with previous study which suggested that smaller particle size entailed greater mass transfer to membrane surface.[23] However, the change in PSD over the course of filtration process reflected the growing tendency of concentration polarisation and fouling formation as a result of particle size increase as observed in Fig. 3. PSD in all trials shifted to the right indicating the aggregation of small Xanthan particles into larger ones. The differences in shifting degrees between trials further explained different Xanthan recovery obtained at each trial. Trial 1 and 4 which displayed the biggest shift of PSD were more difficult to penetrate the pores due to their greater particle size growth, whereas trial 8 experienced the slightest shift of PSD thus associated to low and higher recovery respectively.

There was only a single peak appearance attributed to Xanthan gum from PSD analysis of per-

Table 5 – *PSD of several trial conditions at various solution chemistry*

Trial	Feed				Retentate				
	pH	ZP (mV)	K (mS/cm)	mean volume diameter (nm)	pH	ZP (mV)	K (mS/cm)	mean volume diameter (nm)	total resistance, R_t ($\times 10^{-12} m^{-1}$)
1	5.83	–28.2	30.3	60.58	5.0	–23.1	24.9	90.66	6.33
2	6.69	–15.7	60.5	60.92	6.0	–20.5	61.9	77.2	5.85
3	4.95	–17.9	115	65.43	6.0	–15.3	78.4	83.92	6.19
4	5.84	–13	86.7	48.19	6.23	–25.2	56.6	98.09	9.04
5	4.65	–13.4	127	40.89	5.0	–20.5	87.1	73	9.24
6	–	–	–	–	5.0	–22.5	33	108.9	7.27
7	4.86	–14.1	116	60.31	5.0	–21.2	86.8	80.43	6.17
8	6.09	–11.9	24.7	45.59	6.23	–18.4	24.9	55.85	7.89
9	5.6	–21.7	116	44.9	4.14	–21.2	84.1	85.75	10.6

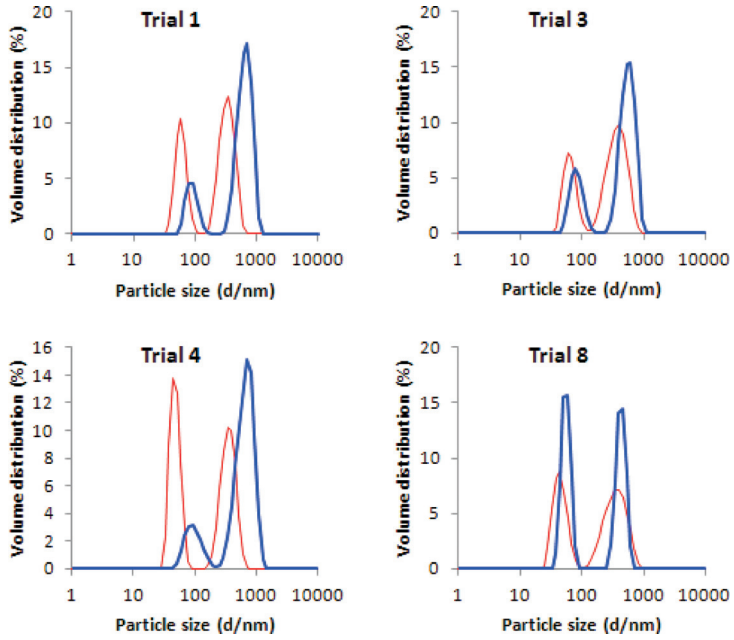

Fig. 3 – *PSD of initial feed sample (red) and retentate (blue) at various trial conditions*

meate samples shown in Fig. 4. This indicates complete oil rejection by membrane surface after the oil droplets underwent complete coalescence process.

Resistance-in-series

Total resistance measured at the end of filtration phase and membrane resistance is shown in Fig. 5. No specific correlation could be drawn from resistance-Xanthan recovery. Nevertheless, there was inverse correlation between particle size and resistance as shown in Table 5; the higher total resistance was observed at larger particle size, contradictory to other studies study which associated higher resistance to smaller particle as a result of

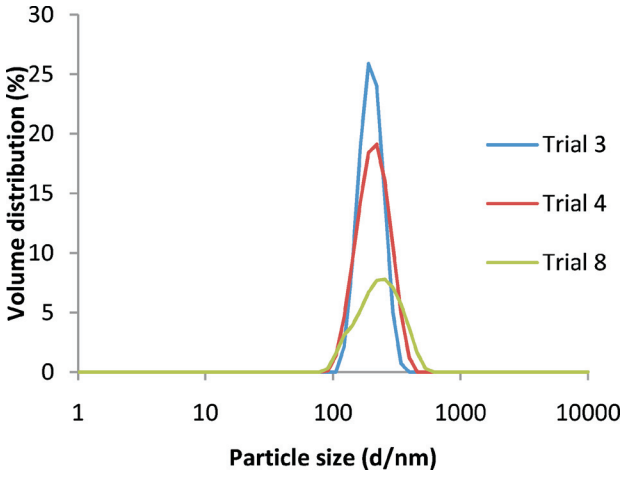

Fig. 4 – *PSD of permeate of several trial conditions*

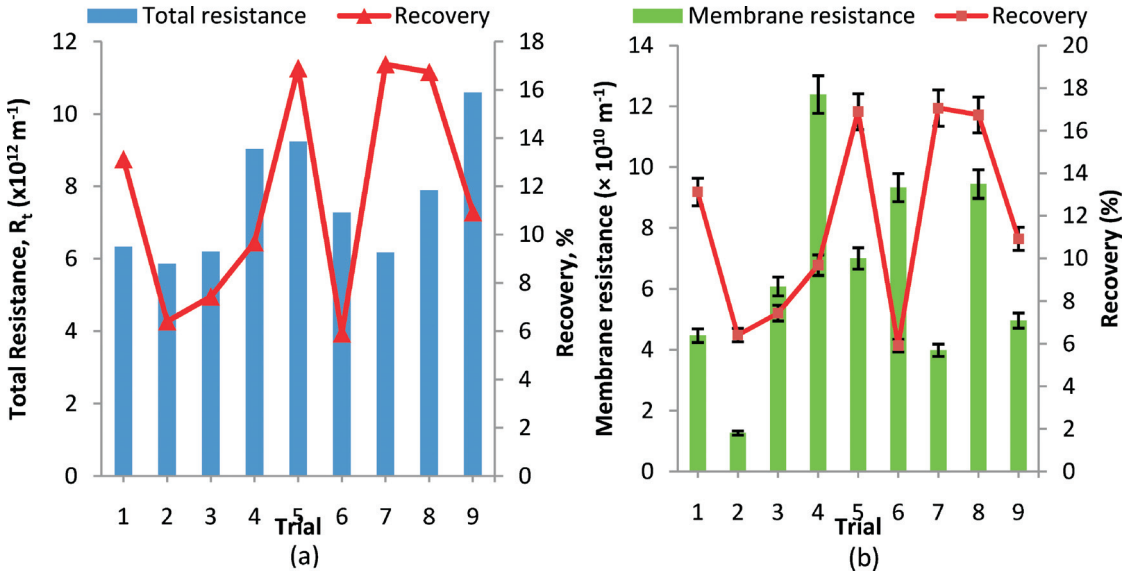

F i g . 5 – *a) Total resistance b) membrane resistance; and recovery of all trial conditions*

greater mass transport and particle deposition on membrane surface leading to faster concentration polarisation and a more compact cake layer.[38] This can be explained by the fact that actual Xanthan molecule exists as a long chain linear structure but DLS measurement had converted the actual Xanthan molecule into spherical equivalent.[39] Long chain linear structure posed greater tendency to form closed-packed cake layer matrix thus particle having larger hydrodynamic diameter equivalent presented greater resistance to XTT due to greater tendency of concentration polarisation formation.

pH and zeta potential (ZP) *analysis*

Particle-particle interaction

Inter-particle interaction that influenced the formation of concentration polarisation and cake layer integrity can be elucidated by ZP analysis based on Derjaguin, Landau, Verwey and Overbeek (DLVO) theory. By comparing trials of similar pH value at retentate side, the higher zeta potential value, which entailed lower total resistance observed in Table 5 was due to greater inter-particle repulsion which reduced the tendency of concentration polarization formation due to loose cake layer integrity. The pH increase which was generally observed towards the end of filtration process might have caused deprotonation of Xanthan's functional group [40], thus stretched Xanthan's molecule into linear conformation as a result of increasing intramolecular repulsion between functional groups within an individual Xanthan molecule. Such phenomenon might further explain the particle size increase generally observed in all trial conditions.

Membrane-Xanthan interaction

The change in solution chemistry is known to influence solute-membrane interaction. Polysulfone was reportedly negatively charged at pH>4 [41] thus most likely to be negatively charged at all pH conditions throughout this study. Cation (K^+) binded to negatively charged membrane surface according to the mechanism laid by other studies and turned membrane surface charge into positive thus becoming attractive to anionic Xanthan as well as shielding repulsive interaction between Xanthan's carboxyl (COO^-) which consistently negatively charged within operating pH as indicated by negative ZP value and membrane's sulfonic acid (SOO^-) functional groups to facilitate XTT.[20,41,42] Thus, the possible mechanism on Xanthan's transmembrane

T a b l e 6 – *L_9 (3^4) Taguchi's orthogonal array and results of Xanthan recovery from aqueous (zero oil) Xanthan broth*

Trial	Factor				Recovery (%)	Ω (db)	SN_L
	A	B	C	D			
1	1	1	1	1	24.29	–4.94	13.87
2	1	2	2	2	44.76	–0.91	–0.78
3	1	3	3	3	44.03	–1.04	0.36
4	2	1	2	3	58.92	1.57	3.90
5	2	2	3	1	40.25	–1.72	4.69
6	2	3	1	2	57.59	1.33	2.47
7	3	1	3	2	46.14	–0.67	–3.45
8	3	2	1	3	36.00	–2.50	7.95
9	3	3	2	1	42.00	–1.40	2.93

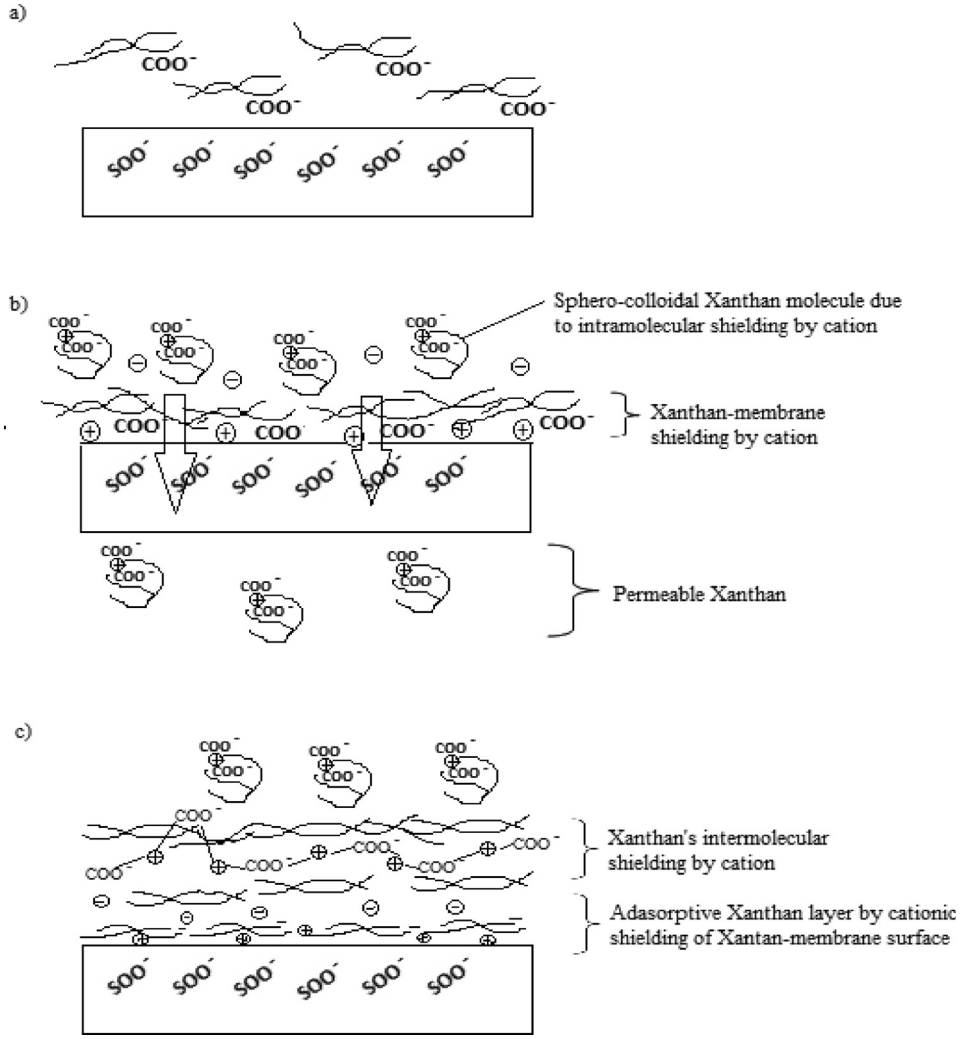

F i g . 6 – *Xanthan transport mechanism Xanthan transport mechanism a) Rejection of Xanthan by membrane due to like-charge repulsion between functional groups b) Xanthan's transmembrane transport at low ionic strength driven by surface's charge modification by cation and membrane-Xanthan shielding by cation c) Formation of secondary cake layer by Xanthan precipitation due Xanthan intermolecular shielding by surplus cation*

transport driven by Xanthan-membrane interaction is illustrated in Fig. 6.

Membrane filtration on zero-oil Xanthan broth

Effect of oil

The effect of oil on Xanthan was analysed using zero-oil broth. Different optimum operating condition was observed for zero-oil broth filtration compared to oily broth filtration as shown in S/N plot in Fig. 7 where the first level of all operating parameters in the latter was optimum. Interestingly, ANOVA result in Table 7 maintained ionic strength as the most significant factor whereas TMP was rendered insignificant. The increased significance of CFV in zero-oil broth filtration was due to the increase effectiveness of hydrodynamic shear to remove cake layer in the absence of oil since oil formed a hydrophobic bond with membrane surface. Furthermore, an earlier

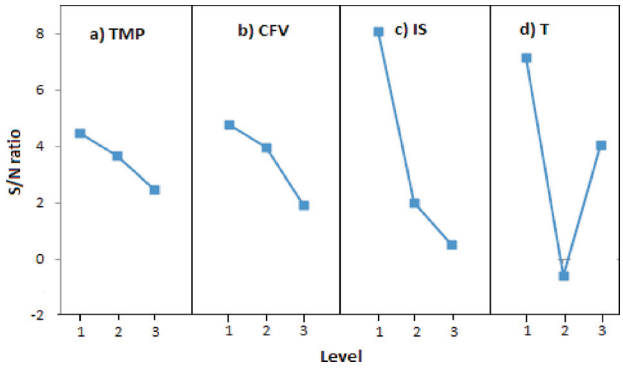

F i g . 7 – *S/N plot of main effect for Xanthan recovery from zero-oil broth a) Transmembrane pressure b) Cross-flow velocity c) Ionic strength d) Temperature*

study which used polysulfone membrane found that hydrodynamic shear was only effective in removing the low oil concentration of oil cake layer [43].

Table 7 – *Result of ANOVA for Xanthan recovery from zero-oil broth*

Factor	SS	DOF	v	F-ratio	F_{cr}	%P
A	(6.10)	(2)		Pooled		
B	12.93	2	6.46	2.12	19	6.25
C	96.46	2	48.23	15.81	19	46.62
D	91.41	2	45.71	14.98	19	44.18
error	6.10	2	3.05			2.95
Total	206.90					100

Only low salt concentration and minimum TMP to bring favourable particle-particle and solute-membrane interactions respectively was necessary to facilitate XTT in zero-oil broth filtration. Previously, a more significant role of TMP during oily broth filtration was required in order to break oil layer and allow Xanthan permeation as evident from complete rejection of oil indicated by the absence of palm oil constituents of GC-MS analysis of permeate (Fig. 10) and single peak appearance of PSD in permeate solution (Fig. 4).

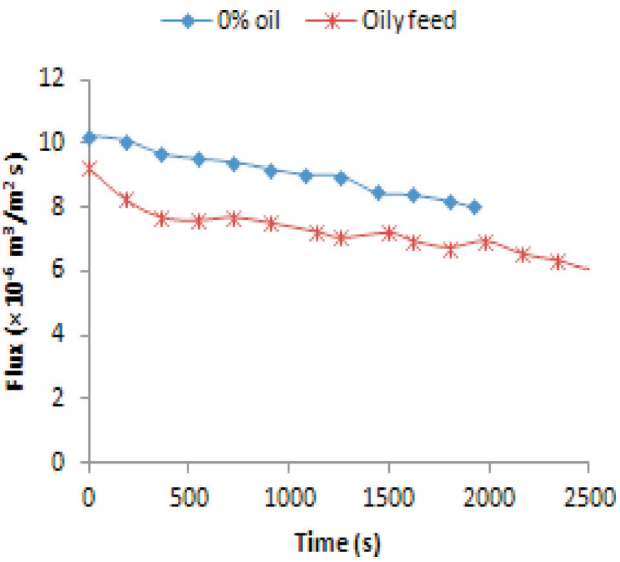

Fig. 8 – *Permeate flux of zero-oil and oily broth both filtration at trial 1 condition*

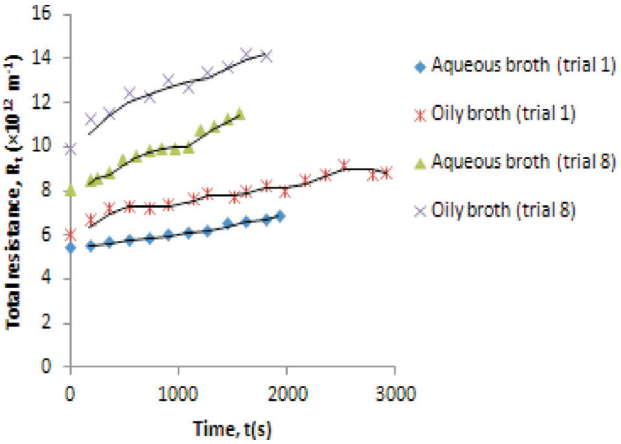

Fig. 9 – *Total resistance vs t plot of trial 1 and trial 8 conditions during zero-oil and oily broth filtration*

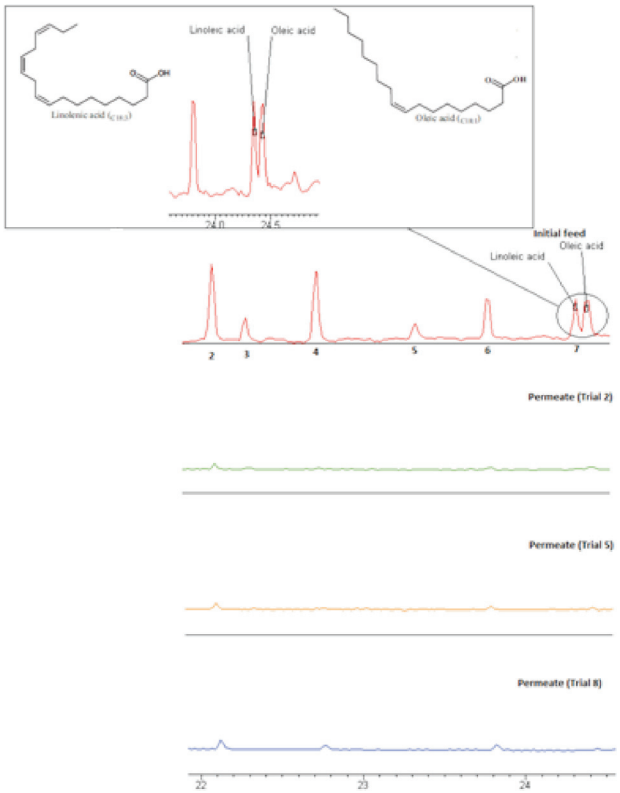

Fig. 10 – *Mass spectrometer (MS) peak of initial feed containing oil and MS of permeate samples of several trial conditions*

Resistance in series model

R_t vs t plot in Fig. 9 shows the downward concavity of both trial 1 and trial 8 of oily broth filtration curve which agreed well with RIS model for cake layer formation. On the other hand, zero-oil broth curve displayed upward concavity, indicating the significant presence of oil cake layer in the former.

Purity analysis by GC-MS

Xanthan's purity was determined by the presence of fatty acids; oleic and linoleic acid in permeate, marked by peak no. 7 in Fig. 10.[44, 45] None of the permeate sample contained fatty acid residue, indicating high purity of Xanthan.

Conclusion

The feasibility of hollow fibre MF to carry out cell and separation as a part of the Xanthan recov-

ery process from palm oil based fermentation broth had been demonstrated by Xanthan recovery at 64 % using optimum condition determined by Taguchi method which was found at level 2 of TMP, ionic strength and temperature and level 1 of CFV. The significance of factor determined by ANOVA was in the following order; IS > TMP > T > CFV. Taguchi method results were later elucidated by analysis on PSD, pH and zeta potential which showed the influence of pH and cation concentration on intramolecular and intermolecular interaction of Xanthan's functional group affecting Xanthan's particle size and Xanthan-membrane interaction.

The oil cake layer that turned out as the limiting factor for better Xanthan permeation was indicated by the significance of CFV during zero-oil broth filtration, which was otherwise undermined by the effect of hydrophobic oil cake layer during oily broth filtration. Oil cake layer was also responsible for lower flux and agreement to RIS's cake layer fouling mechanism as well as the absence of palm oil constituent in permeates after being rejected by oil cake layer.

Nomenclature:

A – Effective membrane area (m^2)
ANOVA – Analysis of variance
C_F – Xanthan concentration in feed
C_F – Xanthan concentration in feed
CFV – Crossflow velocity
CI – Confidence interval
C_P – Xanthan concentration in permeate
DLS – Dynamic light scattering
DLVO – Derjaguin, Landau, Verwey and Overbeek
DOE – Design of experiment
DOF – Degree of freedom
F – F-ratio
F_{cr} – Critical F-ratio
GC-MS – Gas chromatography-mass spectrometry
IPA – Isopropanol alcohol
IS – Ionic strength
MF – Microfiltration
n – number of repetition
NF – Nanofiltration
O/W – Oil-in-water
OA – Orthogonal array
p – fractional percentage value
P – Percent contribution (%)
P_{feed} – Feed pressure
$P_{permeate}$ – Permeate pressure
$P_{retentate}$ – Retentate pressure
PSD – Particle size distribution
R – Xanthan recovery (%)
RIS – Resistance-in-series
R_t – Total resistance (m^{-1})
S/N – Signal-to-noise ratio
SS – Sum of squares
t – Filtration time (s)
TMP – Transmembrane pressure
UF – Ultrafiltration
V – Permeate volume (m^3)
v/v – volume/volume (%)
v_e – variance of error
W/O – Water-in-oil
w/v – mass/volume (%)
XTT – Xanthan's transmembrane transport
y_i – Response's value at *i*th trial
Y_{opt} – Optimum Xanthan recovery
ZP – Zeta potential (mV)
$\overline{T}$ – Average result (Xanthan recovery)
$\overline{A}_i, \overline{C}_j, \overline{D}_k$ – Average response of the significant factors at their respective optimum level *i*, *j*, *k*
μ – Viscosity (Pa s)
Ω – Omega term

References

1. *Zhao, S., Kuttuva, S. G., Ju, L.-K.*, Bioprocess. Eng. **20** (1999) 313–323.
2. *Barbara, K.*, Polym. Degrad. Stab. **59** (1998) 81–84.
3. *Rosalam, S., England, R.*, Enzyme Microb. Technol. **39** (2006) 197–207.
4. *Amanullah, A., Tuttiett, B., Nienow, A.W.*, Biotechnol. Bioeng. **57**(2) (1998) 198–210.
5. *Lu-Kwang, J.*, Bioprocessing for Value-Added Products from Renewable Resources, Y. Shang-Tian, Elsevier, Amsterdam, 2007
6. *Lu, K.J. Su, Z.*, Biotechnol. Tech. **7**(7) (1993) 463–468.
7. *Hofmann, R., Käppler, T., Posten, C.*, Sep. Purif. Technol. **51**(3) (2006) 303–309.
8. *Isa, M.H.M., Frazier, R.A.Jauregi, P.*, Sep. Purif. Technol. **64**(2) (2008) 176–182.
9. *Moresi, M., Ceccantoni, B., Lo Presti, S.*, J. Membr. Sci. **209**(2) (2002) 405–420.
10. *Moresi, M., Sebastiani, I., Wiley, D.E.*, J. Membr. Sci. **326**(2) (2009) 441–452.
11. *Adikane, H.V., Singh, R.K., Nene, S.N.*, J. Membr. Sci. **162**(1–2) (1999) 119–123.
12. *Beier, S.P., Jonsson, G.,* Sep. Purif. Technol. **53**(1) (2007) 111–118.
13. *Saxena, A., Tripathi, B. P., Kumar, M., Shahi, V. K.,* Adv. Colloid Interface Sci. **145** (2009) 1–22.
14. *Zhou, H., Ni, J., Huang, W., Zhang, J.,* Sep. Purif. Technol. **52**(1) (2006) 29–38.
15. *Dezhi, S., Duan, Z., Li, W., Zhou, D.,* J. Membr. Sci. **146** (1998) 65–72.
16. *Abolfazl, E., Elham, G., Toraj, M.,* Desalination **185** (2005) 371–382.
17. *Dizge, N., Soydemir, G., Karagunduz, A., Keskinler, B.,* J. Membr. Sci. **366** (2011) 278–285.

18. *Chen, J.P., Kim, S.L., Ting, Y.P.,* J. Membr. Sci. **219** (2003) 27–45.
19. *Lim, A.L., Bai, R.,* J. Membr. Sci. **216** (2003) 279–290.
20. *Hesampour, M., Krzyzaniak , A., Nyström a, M.,* J. Membr. Sci. **325** (2008) 199–208.
21. *Idris, A., Ismail, A. F., Noordin, M. Y., Shilton, S. J.*, J. Membr. Sci. **205** (2002) 223–237.
22. *Kuttuva, S.G., Restrepo, A.S., Ju, L.K.*, Appl. Microbiol. Biotechnol. **64** (2004) 340–345.
23. *Nataraj, S., Schomacker, R., Kraume, M., Mishra, I. M., Drews, A.,* J. Membr. Sci. **308** (2008) 152–161.
24. *Lo, Y.-M., Yang, S.-T., Min, D.B.,* J. Membr. Sci. **117**(1–2) (1996) 237–249.
25. Malvern Instruments Limited, *DLS Technical note*, Worchestershire, UK (2007)
26. *Safarzadeh, M.S., Moradkhani, D., Ilkhchi, M. O., Golshan, N. M.*, Sep. Purif. Technol. **58** (2008) 367–376.
27. *Ross, P.J.*, Taguchi Techniques for Quality Engineering, 230–250., McGraw Hill, New York, 1996
28. *Chen, H.-L., Chen, Y.-S., Juang, R.-S.*, J. Membr. Sci. **299** (2007) 114–121.
29. *Al-Amoudi, A., Lovitt, R.W.,* J. Membr. Sci. **303** (2007) 4–28.
30. *Chakrabarty, B., Ghoshal, A.K., Purkait, M.K.,* J. Membr. Sci. **325** (2008) 427–437.
31. *Mohammadi, T., Esmaeelifar, A.*, J. Membr. Sci. **254** (2005) 129–137.
32. *Torrestiana-Sanchez, B., L. Balderas-Luna, De. la Fuente, E. B., Lencki, R. W.*, J. Membr.Sci. **294** (2007) 84–92.
33. *Van den Brink, P., Zwijnenburg, A., Smith, G., Temmink, H.,Van Loogrecht, M.*, J. Membr. Sci. **345**(1–2) (2009) 207–216.
34. *Knutsen, J.S., Davis, R.H.*, J. Membr. Sci. **271** (2006) 101–113.
35. *Li, H., Fane, A. G., Coster, H. G., Vigneswaran, L. S.*, J. Membr. Sci. **217** (2003) 29–41.
36. *Hlavacek, M.*, J. Membr. Sci. **102** (1995) 1–7.
37. *Gönder, Z.B., Kaya, Y., Vergili, I., Barlas, H.*, Sep. Purif. Technol. **70** (2010) 265–273.
38. *Waeger, F., Delhaye, T., Fuchs, W.,* Sep. Purif. Technol. **73** (2010) 271–278.
39. *Li, Q., Xub, Z., Pinnau, I.,* J. Membr. Sci. **290** (2007) 173–181.
40. *Susanto, H., Franzka, S., Ulbricht, M.,* J. Membr. Sci. **296** (2007) 147–155.
41. *Susanto, H., Ulbricht, M.,* J. Membr. Sci. **266** (2005) 132–142.
42. *Burns, D.B., Zydney, A.L.,* J. Membr. Sci. **172** (2000) 39–48.
43. *Abbasi, M., Salahi, A., Mirfendereski, M., Mohammadi, T., Pak, A.,* Desalination **252** (2010) 113–119.
44. *Siang, G.H., Makahleh, A., Saad, B., Ling, B. P.*, J. Chromatogr. A **1217** (2010) 8073–8078.
45. *Aparicio, R.n., Aparicio-Ru´2z, R.n.*, J. Chromatogr. A **881** (2000) 93–104.